Three-Dimensional Analysis of Gas Turbine Combustors

N. K. Rizk* and H. C. Mongia†
General Motors Corporation, Indianapolis, Indiana 46206

To achieve the required performance goals and structural durability of gas turbine combustion systems, a design approach was formulated to guide the development effort of the combustor. The approach combines the capabilities of the analytical tools with well-established empirical correlations. By this means, the impact of systematic modification to the details of the burner is easily determined. The validation effort of the developed model included the utilization of the data obtained for a number of production combustors that significantly varied in design and concept. Fuels used in these combustors included typical aviation fuels such as JP-4 and DF-2 as well as specially prepared high-density fuels. Model validation also involved the application of the model in the development phases of an annular combustor. Several modifications to the dome and primary zone features were proposed in this effort. The predictions of the combustor performance and wall temperatures made using the present approach were found to be in good agreement with the measurements.

Nomenclature

BM	= mass transfer number
D_L	= combustor liner diameter, m
F/A	= fuel/air ratio
F_v	= view factor in radiation
ℓ_b	= beam length in gas emissivity equation
LHV	= lower heating value of fuel, kJ/kg
Lu	= luminosity factor in gas emissivity equation
m_B	= fuel fraction burned in subvolume
m_{ev}	= fuel fraction evaporated in subvolume
P_3	= liner inlet pressure, kPa
PF	= pattern factor
Pr	= Prandtl number
Re	= Reynolds number
SMD	= Sauter mean diameter, m
S_ϕ	= source term in transport equation
T_3	= liner inlet air temperature, K
T_u	= turbulence characteristics term
V	= volume, m^3
$Wa_{3.1}$	= liner air flow rate, kg/s
εg	= gas emissivity
η_c	= combustion efficiency
ρ_a	= air density, kg/m^3

I. Introduction

GAS turbine combustion systems need to be designed and developed to meet many mutually conflicting design requirements, including high combustion efficiency over a wide operating envelope and low NO_x emissions; low smoke and low lean flame stability limits and good starting characteristics; low combustion system pressure loss; low pattern factor; and sufficient cooling air to maintain low wall temperature levels and gradients commensurate with structural durability. The flowfield around and within the combustor liner (see Fig. 1) is quite complex in that it includes swirl, regions of recirculation, fuel injection, atomization, fuel evaporation, mixing, turbulent combustion, soot formation/oxidation, and convective and radiative heat transfer processes. The phenomenological understanding of these processes is not well established, and the relevant nonlinear coupled transport equations are difficult to solve.

The combustor design and development process has been empirically based with limited help from multidimensional calculations. A number of correlations have been used by combustor designers to help during the design and development activities. Many researchers[1-4] have proposed semiempirical correlations for gaseous emissions, smoke, lean blowout, ignition, pattern factor, and combustion efficiency. Professors Lefebvre and Mellor have developed very useful correlations that can be used for scaleup, for data correlations, and for providing some insight. These correlations or their variants are being used by the gas turbine industry.[5,6]

The empirical/analytical combustor design methodology introduced by Mongia and Smith[7] has been used for designing a number of gas turbine combustors[8,9] The multidimensional calculations provide a good understanding of combustor internal flowfield and therefore can be used for guiding a combustor design process. However, because of our incomplete understanding of the various combustion processes and numerical diffusion, the three-dimensional calculations for practical gas turbine combustors cannot be considered quantitatively accurate.[10-12] Although some progress is being made in further improving the numerics and combustion models,[13] considerably more effort is needed to achieve the model predictive capability required for accurately predicting combustor performance parameters including radial profile, combustion efficiency, smoke and gaseous emissions, and wall temperature levels and gradients. Still further work will be

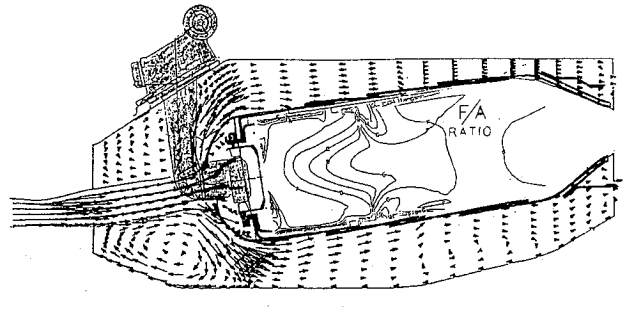

Fig. 1 Model predictions of flowfield around and within combustor.

Presented as Paper 89-2888 at the AIAA/ASME/SAE/ASEE 25th Joint Propulsion Conference, Monterey, CA, July 10-12, 1989; received Aug. 17, 1989; revision received Dec. 15, 1989.

*Staff Research Scientist, Allison Gas Turbine Division. Member AIAA.

†Chief Combustor R & D, Allison Gas Turbine Division. Member AIAA.

needed to predict pattern factor, ignition, and lean blowout (LBO) characteristics.

The development of an alternative approach, as outlined in Ref. 14, over the last four years has been described in recent publications.[15-17] In this approach we combine three-dimensional finite volume calculations with macrovolume expressions extended from Refs. 1 and 2 to yield "bottom-line" quantities of interest to combustion design engineers. A description of the three-dimensional performance model is given in Sec. II and followed by validation in Sec. III. How this approach can be used for combustor design and development purposes is illustrated in Sec. IV and followed by a summary in Sec. V.

II. Three-Dimensional Combustor Performance Model

An essential requirement of the combustor modeling activity is to predict the performance of the combustor with reasonable accuracy. As a result of the complexity of the combustor geometry, often it is difficult to adopt a typical empirical design approach to achieve significant advances in technology. On the other hand, the successful simulation of the actual combustor hardware by using the analytical models requires significant improvement of their physical submodels and numerical techniques.

An approach based on both analytical and empirical considerations has been formulated and validated with gas turbine combustor data over the past several years. The approach comprises the following steps: 1) multidimensional computation of combustion and flow characteristics of a combustor sector; 2) evaluation of relevant parameters within each volume unit of the sector; and 3) utilization of empirical correlations in determining the relative contribution of each subvolume to overall combustor performance.

A. Multidimensional Computation

A three-dimensional variable, finite-difference code that solves the Navier-Stokes equations for a reacting flowfield is adopted in the present approach.[18] The program simulates turbulence by the two-equation K-ε model,[19] and combustion following vaporization is determined by a two-step chemical reaction model based on Arrhenius and eddy breakup concepts.[20,21]

The transport equations for all dependent variables are of the following form:

$$\text{div}[\rho \boldsymbol{u}\phi - (\mu_{\text{eff}}/P_r)\,\text{grad}\,\phi] = S_\phi \qquad (1)$$

where ρ is mixture density, $\boldsymbol{u}$ is the velocity, μ_{eff} is effective turbulent viscosity, P_r is the effective Prandtl/Schmidt number, and $S\phi$ is the source term for variable ϕ. The following variables are computed by the three-dimensional code: 1) axial, radial, and swirl velocity components; 2) specific enthalpy and temperature; 3) turbulence kinetic energy and dissipation rate; 4) unburned fuel and composite fuel fraction; and 5) fuel spray trajectory and evaporation rate.

An iterative finite-difference solution procedure is used to solve the resulting system of nonlinear, partial differential equations. Extensive improvements in the code included the development of a more flexible grid system and the incorporation of an evaporation model extended to address the relevant properties of a wide range of fuel types. A modified form of spray drop size distribution that has been found to more accurately fit experimentally measured distribution[22,23] was also included in the three-dimensional program.

B. Combustor Subvolumes Flow Evaluation

Modeling of the gas turbine combustor involves the selection of a representative sector of the combustor that includes details of the front end configuration and radial injection features. Provisions made in the design to supplement the cooling of the combustor wall are also simulated in the combustor sector. Typically, the sector is divided into a large number of finite-difference nodes along axial, radial, and circumferential directions of the order of 25,000 total nodes or even higher if necessary.

To use the output data of the three-dimensional code in the developed analytical-empirical approach, a feature is introduced into the code that allows the modeled combustor sector to be divided into a relatively large number of subvolumes. Each subvolume is individually considered, and its contribution to the combustor overall performance is added to those of other subvolumes according to the criteria described later in this section. A sensitivity study on the optimum number of subvolumes needed in the calculation was performed by gradually increasing the number until no significant changes in the results were noticed. In the present approach, a total number of around 800 subvolumes is considered sufficient to represent the whole combustor in the calculations. By this means, sophisticated reacting flow models are brought closer in representing actual combustor hardware with significantly less computation.

The relevant combustion and flow characteristics within each subvolume are evaluated and prepared for use as an input to the performance correlations. The three-dimensional code provides these data that include gas flow rate, flow averaged gas temperature, fuel/air ratio, fractions of fuel evaporated and burned in each subvolume, in addition to the turbulence kinetic energy and its dissipation rate.

The overall performance of the combustor is obtained by the summation of the contribution of each subvolume to the corresponding performance parameter. The fraction of fuel burned, that indicates the level of reaction activity, is used to weigh relative contributions from various subvolumes. Volume fraction of the subvolume unit is, in some instances, used as a weighting factor whenever the performance parameter under consideration is not directly related to the fuel/air reaction, but rather by the mixing rate in the combustor.

C. Combustor Performance Calculation

The performance of the gas turbine combustor is largely governed by the residence time in the combustion zone, evaporation of fuel spray, reaction, and mixing rates. As discussed earlier, semiempirical correlations have been used successfully in the design and development phases of the combustor. The combustor is treated in these correlations either as a single reactor or as a number of reactors representing various combustion and dilution zones.

A notable example of the application of the semiempirical approach to evaluate the influence of fuel properties on combustor performance is illustrated in Refs. 1 and 2. A vast amount of data obtained for a number of production engine combustors was employed to reach quantitative relationships that gave satisfactory correlation with the data. The success of this approach relies on the accurate estimation of the liner volume occupied in combustion and the fraction of the total air used in primary zone combustion. Average values of gas properties in the combustion zone are considered in the calculation, and rate of mixing is taken to be directly proportional to liner pressure loss.

The capability of these correlations to match closely the combustor performance data indicates that the correlations embody most of the key parameters governing the operation of the combustor. The main variables involved in deriving each expression were examined and carefully redefined in the present approach to enable merging into the design system. By this means, the need to make the engineering estimates of the aforementioned parameters based on available data is eliminated because the three-dimensional combustor model clearly describes the flowfield and various combustion processes. Thus, the present approach could be applied to predict the performance of current as well as new combustors.

The calculation procedure adopted in the performance model involves a number of subsequent steps. First of all,

a three-dimensional analysis of the combustor flowfield is performed to provide the detailed information needed for the performance calculations. Figure 2 illustrates the grid network used in the analysis of some of the combustors. The continuous lines shown in this figure define the boundaries of the selected subvolumes in this case. This step is followed by the evaluation of the combustion and flow characteristic within each subvolume of the combustor. Finally, the semiempirical correlations are used to evaluate the relative contribution of each subvolume to the overall combustor performance parameters using the criteria described in the previous subsection.

The expressions used to predict emissions in the combustor performance model are given as follows:

$$\mathrm{CO(g/kg)} = \frac{A_1}{P_3^{1.5}}\left[\frac{m_A m_B T e^{-0.0023T}}{V(1-m_{ev}/m_F)T_u^{0.5}}\right]_{ijk} \tag{2}$$

$$\mathrm{UHC(g/kg)} = \frac{A_2}{P_3^{2.5}}\left[\frac{m_A m_B T e^{-0.0025T}}{V(1-m_{ev}/m_F)T_u^{0.5}}\right]_{ijk} \tag{3}$$

$$\mathrm{NO_x(g/kg)} = A_3 P_3^{1.25}\left[\frac{V m_B e^{0.003T}}{T m_A}\right]_{ijk} \tag{4}$$

The exhaust smoke produced by the combustion system represents the balance between the formation process in fuel-rich zones that typically exist in the primary zone and the soot oxidation in the intermediate zone and possibly the dilution zone. The expressions used to predict the soot formation and oxidation are given by

$$S_F(\mathrm{mg/kg}) = A_4 P_3^2 (18-H)^{1.5}\left[\frac{(F/A)m_B}{T m_A T_u^{0.25}}\right]_{ijk} \tag{5}$$

$$S_0(\mathrm{mg/kg}) = A_5 \frac{P_3^2}{V}\left(\frac{F/A}{T}\right)_{pz}\left[\frac{V e^{0.0011T}}{m_A(F/A)}\right]_{ijk}(18-H)^{1.5} \tag{6}$$

The subscript pz indicates average values in the primary zone, and H is the weight percentage of hydrogen in fuel.

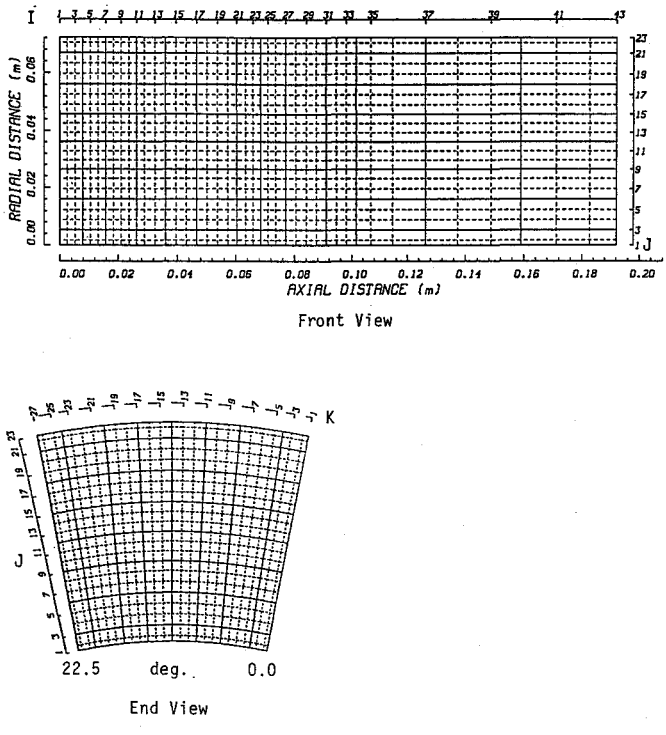

Fig. 2 Grid network used in the three-dimensional analysis.

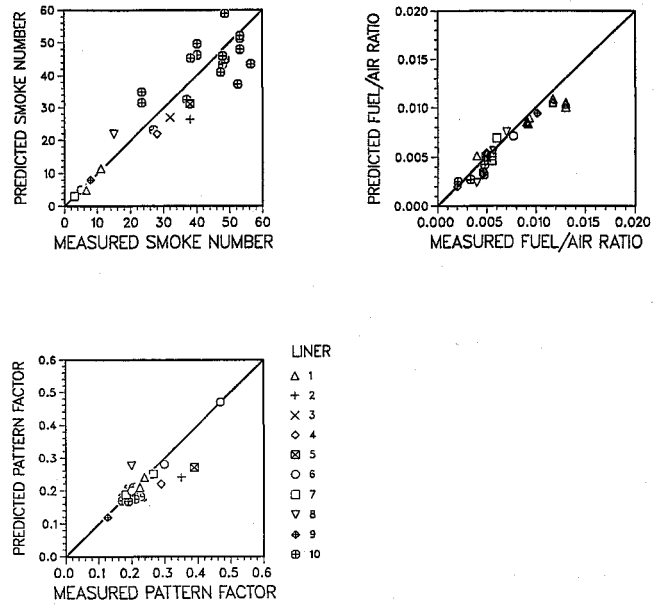

Fig. 3 Comparison between predicted and measured smoke, LBO *F/A* ratio, and *PF*.

The combustion efficiency calculation is based on reaction, evaporation, and mixing rates considerations as follows:

$$\eta_c = \eta_r \eta_{ev} \eta_{mix} \tag{7}$$

where

$$\eta_r = 1 - \exp\left(-A_6 P_3^{1.3}\left[\frac{V m_B e^{T/400}}{m_A}\right]_{ijk}\right) \tag{8}$$

$$\eta_{ev} = 1 - \exp\left(-A_7\left[\frac{m_F m_B}{m_A}\right]_{ijk}\right) \tag{9}$$

$$\eta_{mix} = 1 - \exp\left(-\frac{A_8}{V}[T_u^{0.5} V]_{ijk}\right) \tag{10}$$

The correlation developed to predict the combustor exhaust gases pattern factor uses the turbulence characteristics of flow that govern the mixing rate in various zones of the combustor, the length occupied in fuel evaporation L_{ev}, and an equivalent length of combustor that accounts for the transition section of liner L_L. The pattern factor is given by

$$PF = 1 - \exp - A_9 \Big/ \left(\frac{L_L - L_{ev}}{D_L V}[T_u^{0.5} V]_{ijk}\right) \tag{11}$$

In the above equations, the expressions within the square brackets are provided by the three-dimensional combustor model and summed over each of the control volume units. T is gas temperature, m_A is air flow rate, V is volume, and m_F is fuel flow rate. Fuel mass fractions evaporated and burned within each subvolume are represented by m_{ev} and m_B, respectively. The mass fraction m_B provides a means to govern the contribution from each unit to the overall combustor performance. T_u is a parameter to describe mixing rate and is proportional to the eddy diffusivity, mixing area, and density gradient. It is given in terms of the turbulence characteristics within each subvolume as follows:

$$T_u = [\rho_a K^{1.5}/(\varepsilon/K)^2]_{ijk} \tag{12}$$

where K is kinetic energy of turbulence, ε is its rate of dissipation, and ρ_a is gas density.

In order to use the three-dimensional calculations in predicting the fuel/air ratio at LBO, the evaporation characteris-

tics at the conditions employed in the three-dimensional analysis are converted into the corresponding characteristics at the LBO conditions through a parameter t_r. This parameter is based on the ratio of the evaporation times at the two operating conditions and determined from the evaluation of the values of the spray Sauter mean diameter (SMD) and the evaporation constant (λ_{ev}). The SMD is calculated using appropriate equations for both airblast and pressure atomization modes.[24] Combined mode is also considered whenever a dual fuel circuit atomizer is employed in the combustor, provided that the fuel at LBO requires the operation of both circuits.

The λ_{ev} calculation is based on the vapor concentration gradient concept that estimates the gas properties at reference film temperature using the one-third rule of the following form[25]:

$$T_r = T_s + (1/3)(T_\infty - T_s) \tag{13}$$

T is the temperature, and subscripts r, s, and ∞ refer to reference, surface, and ambient conditions. The fuel vapor concentration is evaluated using the vapor partial pressure principle that is based on the mass transfer number (BM). The evaporation calculation takes into account both heat-up and steady-state stages in addition to the forced convection effects. The evaporation constant λ is given by

$$\lambda = \frac{8kg}{C_{pg}\rho_F}\ell n(1+BM)(1+0.3R_e^{0.5}P_r^{0.33}) \tag{14}$$

Re and Pr are the Reynolds and Prandtl numbers based on gas properties at film temperature, relative velocity, and instantaneous drop diameter, kg, C_{pg}, and ρ_F are thermal conductivity, specific heat of gas, and fuel density, respectively. The calculation follows a step-by-step procedure throughout the life of the droplet to determine the effective evaporation constant λ_{ev}.

Because the fuel/air ratio at LBO conditions is not known in advance, the values of the SMD and λ_{ev} are calculated at an assumed value of LBO fuel/air ratio and used to determine the evaporation time ratio t_r. The calculated LBO fuel/air ratio is given by

$$\text{LBO } F/A = \frac{A_{10}}{\text{LHV}} P_{3des}\left(\frac{FW_{a3}t_r}{P_3^{1.3}e^{T/300}}\right)\left[\frac{m_{ev}m_B}{Tm_A m_F}\right]_{ijk} \tag{15}$$

F is the fraction of air based on the average fuel/air ratio in the primary zone, and P_{3des} is the system pressure used in the three-dimensional analysis. The assumed LBO F/A ratio is then gradually changed in small increments, and the procedure is repeated until the calculated LBO F/A falls within a prescribed range around the assumed value. A_1 to A_{10} are empirical constants that are fixed for all combustor configurations. Their values are 0.0093, 3.85, 15, 0.1773, 0.042, 0.07, 1.71, 1500, 0.0095, and 98,000, respectively.

A model to calculate the ignition fuel/air ratio, based on the quench distance concept,[1] has been applied to a limited number of configurations. The details of this model and its application to evaluate the effects of the high-density fuels on combustor performance are given in Ref. 17.

D. Combustor Wall Temperature Calculation

In a practical combustion system, the liner walls are heated by the radiation from the flame, hot gases, and convection from the gas flow within the chamber. The removal of heat from the burner walls occurs through radiation to the outer casing and convection to the annulus air. The removal of heat is usually supplemented by one of the well-established cooling concepts available for gas turbine combustor. This step is necessary to maintain acceptable levels of liner wall temperature and gradients through operation to meet the durability goals of the combustor.

Because of the complexity involved in estimating the luminous emissivity from the knowledge of the size, mass concentration, and optical properties of the soot particles in the flame, a luminosity factor L_u is introduced into the empirical expression of nonluminous flame as follows[24]:

$$\varepsilon g = 1 - \exp(-290P_3L_u(F/A\ell_b)^{0.5}T_g^{-1.5}) \tag{16}$$

The factor L_u depends largely on such parameters as carbon/hydrogen mass ratio and fuel hydrogen content. A widely used equation is given by[24]

$$L_u = 0.0691(C/H - 1.82)^{2.71} \tag{17}$$

However, an expression that was found to fit a wide data base is employed in the present approach and given as follows[17]:

$$L_u = 5.964 \times 10^8/H^{7.365} \tag{18}$$

The beam length ℓ_b is determined by the size and shape of the gas volume. To obtain more accurate estimates of liner wall temperature, it is essential to include the radiation flux contribution from various combustor zones into each wall segment. This step calls for the knowledge of the detailed three-dimensional combustor flowfield in addition to an accurate means of defining a radiation view factor F_v. Adopting this concept, the radiation flux to a wall segment can be calculated using the following equation:

$$R = 0.5\sigma(1+\varepsilon_w) \times \sum[F_v\varepsilon_g T^{1.5}(T^{2.5} - T_w^{2.5})]_{ijk} \tag{19}$$

where the terms within the square brackets are based on local properties within each combustor zone, as given by the three-dimensional code. The ε_w is wall emissivity, and σ is the Stefan-Boltzmann constant. The calculation of the wall temperature T_w is performed by balancing the heat fluxes on a wall segment through an iterative procedure, and a wall conduction component is used to determine the temperature gradient across the segment.

III. Validation

The main objective of the three-dimensional combustor performance model is to make engineering predictions of combustion efficiency, smoke, LBO, pattern factor, CO, unburned hydrocarbons, and NO_x emissions. Over the years, the

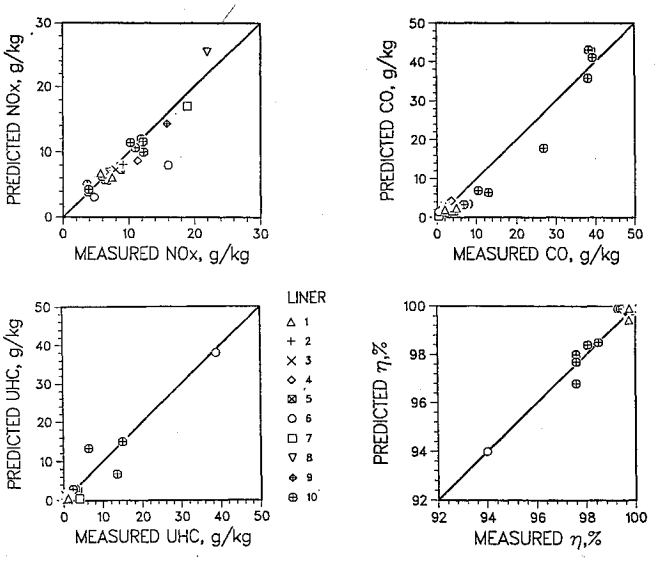

Fig. 4 Comparison between predicted and measured NO_x, CO, combustion efficiency, and UHC.

Table 1 Comparison between measured and predicted design point performance

Combustor configuration	Baseline		Mod I		Mod II		Mod III		Final low-smoke comb	
	M[a]	P[b]	M	P	M	P	M	P	M	P
SAE smoke no.	38.0	35.5	38.0	30.6	32.0	28.9	28.0	20.3	11.0	11.1
NO_x EI	8.7	10.5	9.1	8.0	NA[c]	7.3	11.4	8.6	7.5	7.4
CO EI	3.6	4.4	2.0	2.3	2.0	2.3	3.6	2.8	1.9	1.9
UHC EI	0.8	0.9	1.2	1.2	0.4	1.2	NA	0.9	1.2	1.0
Pattern factor	0.39	0.38	0.40	0.21	0.35	0.33	0.29	0.23	0.24	0.24

[a]M = measured. [b]P = predictions. [c]NA = not available.

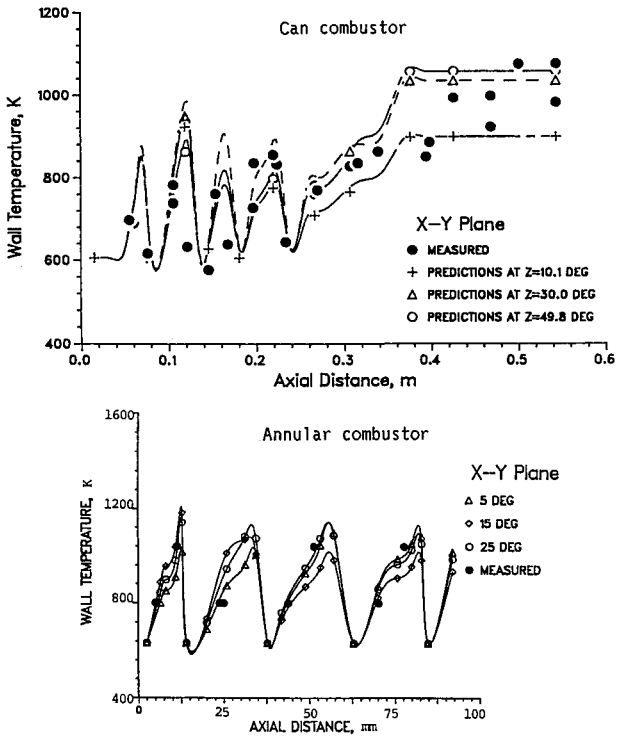

Fig. 5. Comparison between predicted and measured wall temperatures.

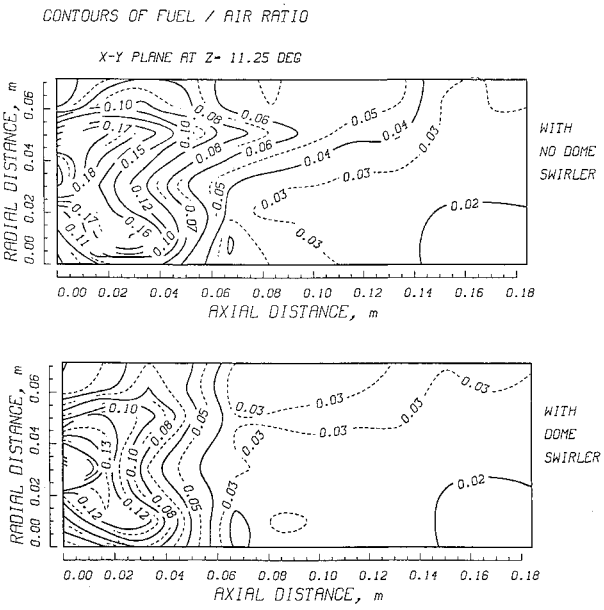

Fig. 6 Effect of dome design on fuel/air ratio distribution.

model has been validated with data on ten different combustors that encompass can, straight throughflow, and reverse flow combustors. Six of these combustors burn DF-2, two use JP-4, and the other two use JP-5. One combustor (identified as liner 10 in Figs. 3 and 4) was tested with JP-4 and four high-density fuels.

The measured data from ten combustors were used to validate the set of the empirical constants A_1 to A_{10} that was determined from the analysis of a limited number of combustors under varying operating modes. Figures 3 and 4 show comparison between predicted and measured Society of Automotive Engineers smoke number, LBO fuel/air ratios, pattern factor, NO_x, CO, unburned hydrocarbons, and combustion efficiency.

The agreement between predictions and data is quite good indicating that the three-dimensional combustor performance model is capable of accurately predicting the design performance parameters. The model in addition to providing physical insight into the various gas turbine processes gives quantitatively accurate tradeoffs between often conflicting design requirements, e.g., the groupings of Figs. 3 and 4.

The capability of the developed heat transfer concept in predicting the wall temperature of the combustor is illustrated in Fig. 5. Two examples are shown in the figure for both can and annular combustor configurations. The first combustor is convection/film cooled liner, whereas the other one is built with a machined ring construction. The predictions of the wall temperature in an axial plane in line with the fuel injector are plotted together with the measured data. Both thermal paint and thermocouple techniques were used to obtain the data. Once again, good agreement is obtained between the calculated and measured wall temperatures. The method, therefore, could be used effectively to reach the optimum cooling distribution using the same amount of cooling air available in the design.

IV. Application

The three-dimensional combustor performance model has been found very useful as a design tool during both combustor design and development process. In this section we show as an example how the model was used for reducing the smoke emissions of a production annular combustor with the following nominal combustor flow conditions at the design point: 1) combustor inlet pressure = 1110 kPa; 2) combustor inlet temperature = 618 K; 3) air flow rate = 16.2 kg/s; and 4) combustor outlet temperature = 1491 K.

A number of minor combustor modifications were investigated on a full-scale combustor rig in order to reduce the smoke emissions without adversely affecting other performance parameters and liner wall temperature levels and gradients. The baseline combustor with the computed primary zone air flow split of 23% has no dome swirlers; whereas the final low-smoke configuration uses dome swirlers in addition to increasing the primary zone air to 29.0%.

In addition to the baseline (without dome swirlers) and its final low-smoke configuration (with dome swirlers), three intermediate modifications were experimentally evaluated and

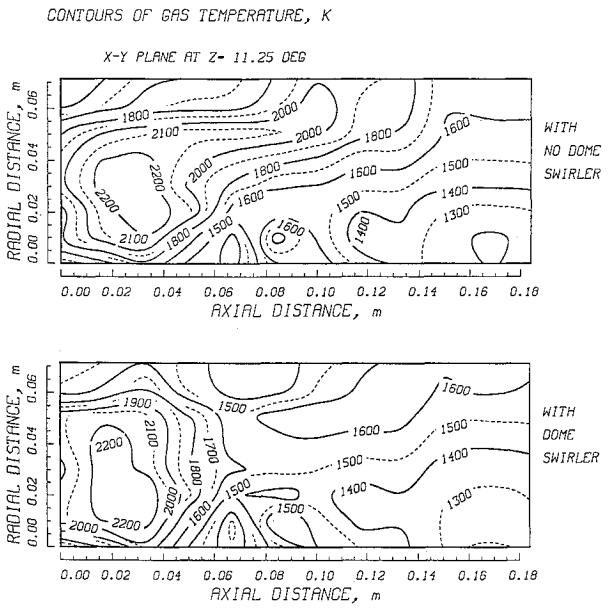

Fig. 7 Influence of dome swirler on gas temperature pattern, K.

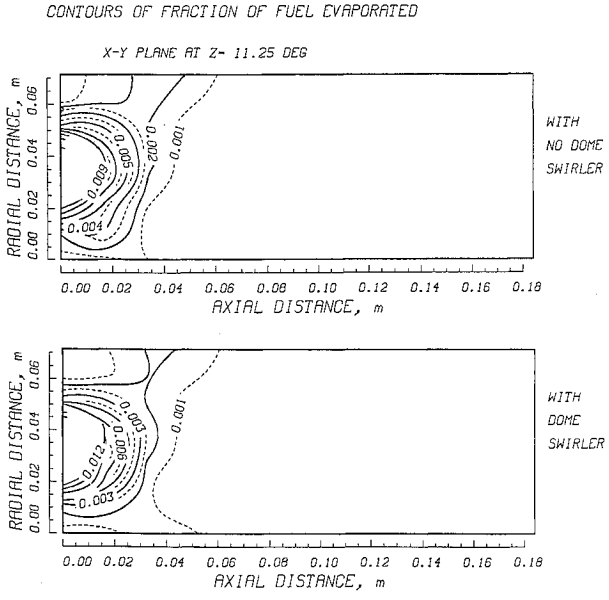

Fig. 8 Contours of fraction of fuel evaporated in the combustor.

compared with the three-dimensional combustor performance model predictions. Table 1 shows comparison between data and predictions for the design point. The model does an excellent job in correlating the measured smoke emissions that range from 38.0 with the baseline to 11.0 with the final low-smoke combustor configuration. Similarly, the agreement is quite good in regard to the gaseous emissions and pattern factor. The model correlation with other performance parameters as well as data at off-design operating points was equally good.

In order to illustrate the capability of the three-dimensional combustor model to detect the differences in the flowfield resulting from the modifications to the liner configuration, examples of the flowfield of the combustor are given in this section. The three-dimensional results of the baseline combustor are compared to those of the combustor that use the dome swirler, using computer drawn plots of a selected longitudinal x-y section of the combustor sector.

Figure 6 shows the contours of the fuel/air ratio for both configurations. The inclusion of the dome swirler in the combustor design has eliminated most of the very rich regions that were responsible for the production of high levels of smoke in the primary zone of the no-dome swirler configuration. An equivalence ratio in excess of 2.0 is found in most of the front end of the combustor, while with the inclusion of the swirler, this occurs only in a very limited region near the fuel injector, which is located approximately in the middle of the channel height. Better mixing is achieved in the primary zone by introducing the swirler that enhances the dispersion and evaporation of spray droplets resulting in much lower fuel/air ratio levels near the liner walls in this critical region.

The corresponding temperature contours for the two configurations are given in Fig. 7. The changes of the fuel/air ratio distribution due to the inclusion of the swirler are reflected on the gas temperature patterns shown in this figure. Regions of higher gas temperature are observed in the baseline design to extend to the dilution zone, especially towards the upper liner wall due to the higher fuel/air ratio in these regions.

The effect of the improved fuel/air mixing in the primary zone, with dome swirler, on the evaporation rate and fuel

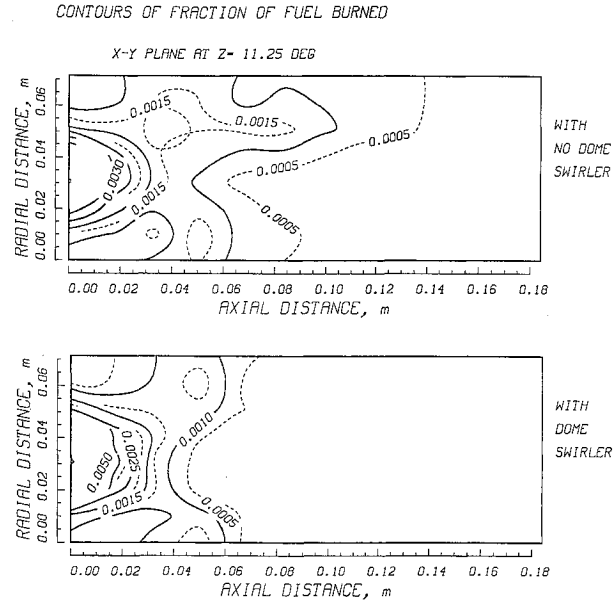

Fig. 9 Effect of dome design on fraction of fuel burned in various zones.

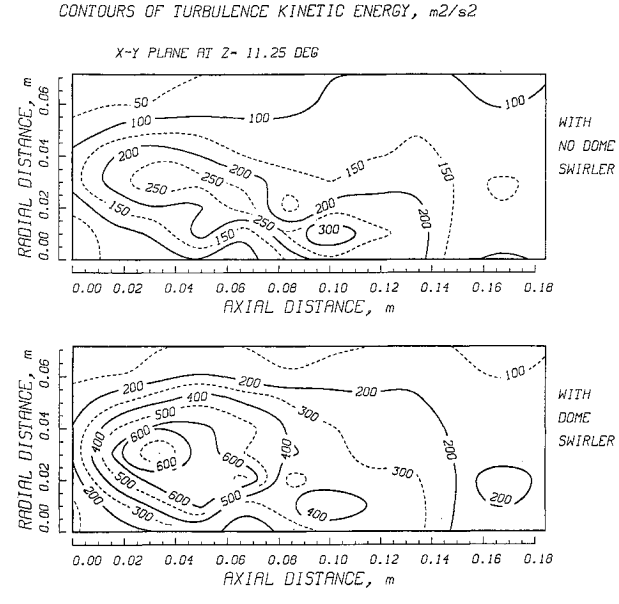

Fig. 10 Kinetic energy of turbulence pattern for both combustor designs, m^2/s^2.

burned contours is illustrated in Figs. 8 and 9, respectively. Inspection of the contour levels indicates that larger fractions of the fuel evaporate and react earlier in the combustor when the swirler is employed in the design. Enhanced mixing and evaporation within the primary zone due to the proper design modifications cause the burning process to be completed earlier in the combustor. A fraction of fuel burned contours are almost nonexistent further downstream of the x-y slice shown in this figure. It is obvious in this x-y plane, which is in line with the fuel injector, that the reaction of the fuel continues over a large portion of the combustor length in the baseline configuration.

Contours of the kinetic energy of turbulence for both combustor configurations are given in Fig. 10. The great influence of the dome swirler on the levels of turbulence in the combustor is obvious in this figure. The significant increase of the kinetic energy of turbulence due to the interaction of the swirler flow and the combustor radial jets has a favorable effect on various mixing and combustion processes within the liner.

It is seen that the information given by the three-dimensional combustor model serves to visualize the impact of systematic modification to the details of the combustor on its performance. The prediction of the combustor performance, in addition to the vast amount of information on the flowfield, will certainly guide the design and development of gas turbine combustors with minimum hardware testing.

V. Conclusion

A three-dimensional performance model that is based on combining the analytical capabilities of combustor codes with well-established empirical correlations has been formulated. The developed design approach was verified by the application of the method to a number of production combustors that varied significantly in design and concept. They represented various classes of can-annular, through, and reverse flow annular combustors. Satisfactory agreement between the model predictions and the experimental data was obtained under various operating conditions.

In the effort to enhance the performance and emissions characteristics of an annular combustor, the details of the dome design and primary zone features were investigated to reach the optimum configuration. This investigation was supported by an intensive hardware testing of a number of configurations under the actual engine operating conditions. In a parallel effort, the design method was employed to evaluate its capabilities to sense the impact of the design modifications on the combustor performance. It was found that the effect of the inclusion of the dome swirler in the combustor design, to improve mixing in the primary zone, is closely predicted by the model. The significant reduction in smoke level produced by the combustor as a result of this modification is well captured in the model.

It is also found that the heat transfer analysis, coupled with the multidimensional combustor codes, provides a very useful means in the selection procedure of the optimum cooling configuration for the combustor.

References

[1]Lefebvre, A. H., "Fuel Effects on Gas Turbine Combustion-Ignition, Stability, and Combustion Efficiency," *Transactions of the ASME, Journal of Engineering for Gas Turbines and Power*, Vol. 107, No. 1, 1985, pp. 24–37.

[2]Lefebvre, A. H., "Fuel Effects on Gas Turbine Combustion-Liner Temperature, Pattern Factor, and Pollutant Emissions," *Journal of Aircraft*, Vol. 21, No. 11, 1984, pp. 887–898.

[3]Plee, S. L., and Mellor, A. M., "Flame Stabilization in Simplified Prevaporizing Partially Vaporizing and Conventional Gas Turbine Combustors," *Journal of Energy*, Vol. 2, No. 6, 1978, pp. 346–353.

[4]Plee, S. L., and Mellor, A. M., "Characteristic Time Correlation for Lean Blowoff of Bluff-Body-Stabilized Flames," *Combustion and Flame*, Vol. 35, 1979, pp. 61–80.

[5]Steele, L. L., Grant, J. R., Harrold, D. P., and Erhart, J. J., "Application of System Identification Techniques to Combustor Post-stall Dynamics," Air Force Wright Aeronautical Lab., Wright-Patterson AFB, OH, AFWAL-TR86-2105, Feb. 1987.

[6]Rizk, N. K., and Mongia, H. C., "Correlations of High Density Fuel Effects," AIAA Paper 89-0216, Jan. 1989.

[7]Mongia, H. C., and Smith, K. F., "An Empirical/Analytical Design Methodology for Gas Turbine Combustor," AIAA Paper 78-998, July 1978.

[8]Mongia, H. C., "Application of Multidimensional Modeling Techniques to the Design and Development of Gas Turbine Combustors," 1982 Air Force Office of Scientific Research, Annual Contractors Meeting, 1982.

[9]Mongia, H. C., Reynolds, R. S., and Srinivasan, R., "Multidimensional Gas Turbine Combustion Modeling: Applications and Limitations," *AIAA Journal*, Vol. 24, No. 6, June 1986, pp. 890–904.

[10]Srinivasan, R., Reynolds, R., Ball, I., Berry, R., Johnson, K., and Mongia, H. C., "Aerothermal Modeling Program: Phase I Final Report," NASA CR-168243, 1983.

[11]Kenworthy, M. J., Correa, S. M., and Burrus, D. L., "Aerothermal Modeling: Phase I Final Report—Volume I Model Assessment," NASA CR-168296, 1983.

[12]Sturgess, G. J., "Aerothermal Modeling: Phase I Final Report," NASA CR-168202, 1983.

[13]Holdeman, J. D., Mongia, H. C., and Mularz, E. J., "Assessment, Development and Application of Combustor Aerothermal Models," *Toward Improved Durability in Advanced Aircraft Engine Hot Section*, edited by D. E. Sokolowski, NASA TM-4087, April 1989.

[14]Rizk, N. K., and Mongia, H. C., "Gas Turbine Combustor Design Methodology," AIAA Paper 86-1531, June 1986.

[15]Mongia, H. C., "A Status Report on Gas Turbine Combustion Modeling," AGARD CP 422, 1988, pp. 26-1–26-14.

[16]Rizk, N. K., and Mongia, H. C., "The Application of Gas Turbine Combustor Design Method," Central States Combustion Institute Meeting, Combustion Inst., Pittsburgh, PA, May 1988.

[17]Rizk, N. K., and Mongia, H. C., "A 3-D Combustor Performance Validation with High Density Fuels," *Journal of Propulsion and Power* (to be published); also AIAA Paper 89-0219, 1989.

[18]Patankar, S. V., *Numerical Heat Transfer and Fluid Flows*, Hemisphere, Washington, DC, 1980.

[19]Launder, B. E., and Spadling, D. B., "The Numerical Computation of Turbulent Flow," *Computational Methods of Applied Mechanical Engineering*, Vol. 3, 1974, pp. 269–289.

[20]Hautman, D. J., Dryer, F. L., Schug, K. P., and Glassman, I., "A Multiple-Step Overall Kinetic Mechanism for the Oxidation of Hydrocarbons," *Combustion Science Technology*, Vol. 25, 1981, pp. 219–235.

[21]Mongia, H. C., and Reynolds, R. S., "Combustor Design Criteria Validation," Vol. III, USARTL-TR-78-SSC, Feb. 1979.

[22]Custer, J. R., and Rizk, N. K., "Influence of Design Concept and Liquid Properties on Fuel Injector Performance," *Journal of Propulsion and Power*, Vol. 4, No. 4, 1988, pp. 378–384.

[23]Rizk, N. K., and Lefebvre, A. H., "Spray Characteristics of Spill-Return Atomizers," *Journal of Propulsion and Power*, Vol. 1, No. 3, 1985, pp. 200–204.

[24]Lefebvre, A. H., *Gas Turbine Combustion*, McGraw-Hill, New York, 1983.

[25]Faeth, G. M., "Current Status of Droplet and Liquid Combustion," *Progress in Energy and Combustion Science*, Vol. 3, 1977, pp. 191–224.